

REPORT DOCUMENTATION PAGE			Form Approved OMB NO. 0704-0188	
Public Reporting burden for this collection of information is estimated to average 1 hour per response, including the time for reviewing instructions, searching existing data sources, gathering and maintaining the data needed, and completing and reviewing the collection of information. Send comment regarding this burden estimates or any other aspect of this collection of information, including suggestions for reducing this burden, to Washington Headquarters Services, Directorate for Information Operations and Reports, 1215 Jefferson Davis Highway, Suite 1204, Arlington, VA 22202-4302, and to the Office of Management and Budget, Paperwork Reduction Project (0704-0188), Washington, DC 20503.				
1. AGENCY USE ONLY (Leave Blank)		2. REPORT DATE 09/07/2005		3. REPORT TYPE AND DATES COVERED Phase I Final Report, 03/07/05 ~ 09/07/05
4. TITLE AND SUBTITLE Embedded Electro-Optic Sensor Network for the On-Site Calibration and Real-Time Performance Monitoring of Large-Scale Phased Arrays			5. FUNDING NUMBERS HQ0006-05-C-7155	
6. AUTHOR(S) Kyoung Yang				
7. PERFORMING ORGANIZATION NAME(S) AND ADDRESS(ES) Opteos, Inc. 1340 Eisenhower Place, Ann Arbor, MI 48108			8. PERFORMING ORGANIZATION REPORT NUMBER	
9. SPONSORING / MONITORING AGENCY NAME(S) AND ADDRESS(ES) U.S. Army Space & Missile Defense Command ATTN: Mr. Robert C. Parks/ USASMDC P.O. Box 1500, Huntsville, AL 35807-3801			10. SPONSORING / MONITORING AGENCY REPORT NUMBER	
11. SUPPLEMENTARY NOTES The views, opinions and/or findings contained in this report are those of the author(s) and should not be construed as an official Department of the Army position, policy or decision, unless so designated by other documentation.				
12 a. DISTRIBUTION / AVAILABILITY STATEMENT Approved for public release; distribution unlimited.			12 b. DISTRIBUTION CODE	
13. ABSTRACT (Maximum 200 words) This final report summarizes the progress during the Phase I SBIR project entitled "Embedded Electro-Optic Sensor Network for the On-Site Calibration and Real-Time Performance Monitoring of Large-Scale Phased Arrays". The main objective of the project is to develop an innovative electric-field sensor network based on an electro-optic field-detection technique (the Electro-optic Sensor Network, or ESN) for the performance evaluation of phased-antenna arrays at the end of their development/production cycle, and furthermore, for onsite test and calibration of deployed large-scale phased arrays. During the Phase I period, Opteos has built a small-scale ESN system for the feasibility demonstration. In the small-scale ESN system, three EO sensors were used. Opteos has also developed modified serial port to directly control the optical switch along with necessary software in order to acquire measurement data from the three EO sensors while the sensors scan over an antenna under test. The performance of small scale of ESN was characterized by mapping two-dimensional field maps on a patch antenna. During the evaluation process, non-uniform channel-to-channel performance of the optical switch has been observed. In order to compensate the non-uniformity, a polarization compensation method has been developed.				
14. SUBJECT TERMS Electro-optic sensor, sensor network, phased array, array calibration, optical switch			15. NUMBER OF PAGES 30	
			16. PRICE CODE	
17. SECURITY CLASSIFICATION OR REPORT UNCLASSIFIED	18. SECURITY CLASSIFICATION ON THIS PAGE UNCLASSIFIED	19. SECURITY CLASSIFICATION OF ABSTRACT UNCLASSIFIED	20. LIMITATION OF ABSTRACT UL	

NSN 7540-01-280-5500

Standard Form 298 (Rev.2-89)
Prescribed by ANSI Std. Z39-18
298-102

Enclosure 1



PHASE I SBIR PROJECT

PHASE I FINAL REPORT

Embedded Electro-Optic Sensor Network for the On-Site Calibration and Real-Time Performance Monitoring of Large-Scale Phased Arrays

Contract Number: HQ0006-05-C-7155

Contracting Agency: Missile Defense Agency

Contractor: Opteos, Inc.

Principal Investigator: Dr. Kyoung Yang

Reporting Period: 03/07/2005 – 09/07/2005




TABLE OF CONTENTS

1. Introduction
2. Major objectives for the Phase I project
3. System configuration
4. Four channel optical switch
5. Design of optical switch control circuit
6. Performance evaluation of optical switch
7. Fabrication of small scale ESN
8. Performance evaluation of the ESN
9. Phase II R&D plan

1. Introduction

This final report summarizes the progress during the Phase I SBIR project entitled "*Embedded Electro-Optic Sensor Network for the On-Site Calibration and Real-Time Performance Monitoring of Large-Scale Phased Arrays*". The main objective of the project is to develop an innovative electric-field sensor network based on an electro-optic field-detection technique (the Electro-optic Sensor Network, or ESN) for the performance evaluation of phased-antenna arrays at the end of their development/production cycle, and furthermore, for onsite test and calibration of deployed large-scale phased arrays.

At the beginning of this Phase I, Opteos has invited Robert C. Parks, a COR for this SBIR project, to discuss and finalize the overall R&D direction for the Phase I SBIR project. As a result of productive discussions, we have agreed that Opteos would focus its effort on several key objectives during this Phase I, including enhancement of the stability of the EO sensor, acquisition of a fiber-optic-based switch, development of optical-switch control electronics, and a small scale feasibility demonstration at the end of Phase I.

Opteos has finalized the small-scale ESN system configuration for the feasibility demonstration during the Phase I of this SBIR project. Also, Opteos has surveyed commercially available optical switches for the Phase I SBIR research and development. We were able to identify three optical switch manufacturers who have such an optical switch product or are capable of producing a customized device. After a thorough comparison, we have selected a switch manufacturer (LIGHTech Fiber Optics, Inc.) and placed the order for a 1×4 optical switch. Based on the assumption of using LIGHTech optical switch, a switch control circuit has been designed. Subsequently, the switch was purchased and Opteos has performed thorough performance test for the optical switch. Particularly, optical properties of the 4 output channels including insertion loss and polarization preservation have been very carefully evaluated.

The optical switch has four output ports. However, one of the output fibers was damaged during transportation. As a consequence, we had to build a small scale ESN of three EO sensors. Miniaturized GaAs tips formed by a wet etching process were used for the EO sensors. Gradient index (GRIN) lenses were used to focus the optical beam from single-mode fiber into the GaAs tip. Opteos has developed a modified serial port to directly control the optical switch along with the necessary software in order to acquire measurement data from the three EO sensors while the sensors scan over an antenna under test. The performance of the small-scale ESN was characterized by extracting two-dimensional field maps on a patch antenna. During the evaluation process, non-uniform channel-to-channel performance of the optical switch has been observed. In order to compensate the non-uniformity, a polarization compensation method has been developed. Also, non-uniformity caused by the uneven loss characteristics of the switch was calibrated.

2. Major objectives for the Phase I project

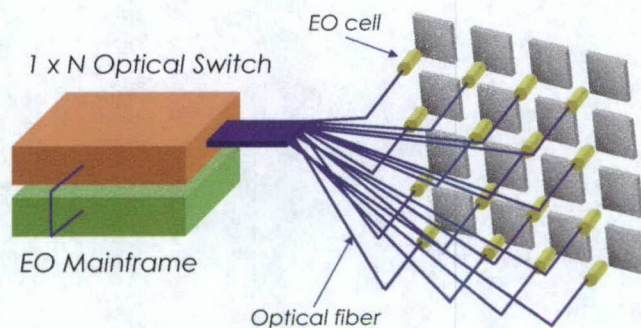


Figure 1. Concept of the electro-optic sensor network (ESN) for onsite applications.

Figure 1 shows the fundamental concept of an ESN specifically designed for onsite array test and calibration applications based on an array with 16 elements. In Fig. 1, one EO sensor is assigned to each antenna in the array in order to monitor the field radiated from that antenna. The collective information from the individual EO sensors will reveal comprehensive information on the operating condition of the array. In the ESN application, the EO mainframe, which is the unit where the optical beam is controlled and the information from sensors converted into electrical signals, needs to support multiple EO sensors for monitoring signals in numerous different locations. In the ESN system, a 1×N optical divider, optical switch, or combination of both may be employed between the output port of the EO mainframe and the EO sensors to realize such a network configuration.

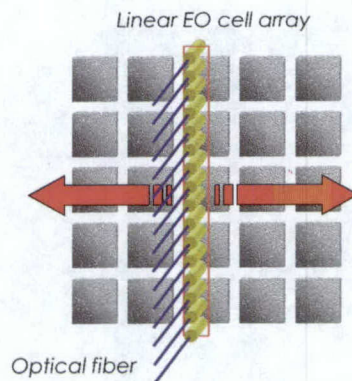


Figure 2. Concept of the ESN in its linear-sensor-array embodiment.

Figure 2 shows an alternative ESN configuration employing a linear arrangement of EO sensors and a linear, mechanical scanning scheme. The ESN configuration shown in Fig.2 would be more versatile to test and characterize arrays under a controlled environment, while the embedded concept shown in Fig. 1 would be an appropriate approach for onsite embedded applications. In fact, the ESN in the linear-sensor-array configuration is expected to become a

valuable test and characterization tool for radar arrays during their design/development process, or even in their final performance validation at the end of production. The concept shown in Fig 2 is the projected prototype ESN system at the end of the Phase II of this SBIR project, while the true embedded scheme shown in Fig. 1 is expected to be developed as a post-SBIR effort. During Phase I, a significant portion of our effort was concentrated on the feasibility demonstration of important elements of the ESN systems. We carefully selected our objectives for the Phase I so that the R&D activities during this phase would be directly used during Phase II independent of the final embodiment of the ESN system.

The exceptional functionality of the EO probe as an electric-field detector has been successfully demonstrated through numerous near-field scanning applications. In particular, due to its extremely broad measurement bandwidth, minimal invasiveness, and immunity from EM interference, the EO sensor can be considered as a near-ideal field detector for embedded or close-proximity electric-field detection for antenna arrays. However, the EO sensor has been originally developed as a field-sensing device for the EO field-mapping system. The EO field-mapping system, an innovative RF characterization instrument, is typically operated under a controlled, indoor environment, and, as a consequence, the EO probe itself was assumed to be used in such a laboratory environment. However, it is apparent that the EO sensors for the ESN application may be exposed to a considerably more harsh environment, particularly in the case of the embedded configuration shown in Fig. 1. As a result, it may be necessary to enhance the stability of the EO sensor, particularly against the potential variations in environmental conditions.

In addition to the EO sensors, the optical-signal-distribution unit will be a vitally important subsystem for the entire ESN system. For optical signal distribution, a $1 \times N$ optical divider, optical switch, or some combination of both could be employed between the output port of the EO mainframe and the EO sensors in order to realize such a network configuration. If the EO mainframe employs an optical divider with multiple photodiodes and signal-processing circuits, it will have the capability to monitor multiple EO sensors simultaneously. However, even though one EO sensor does not require a high level of beam power for its operation (*e.g.*, a GaAs EO probe requires about 7 mW of beam power), the maximum number of EO sensors that one EO mainframe could handle in this case would be largely limited by the beam power. For the Phase I project, we decided to use an optical switch as the main signal-distribution device, since the use of a laser source with higher output power, which would allow the use of optical dividers, would become feasible only during Phase II.

The successful R&D activities during Phase I have allowed Opteos to perform a successful feasibility demonstration based on the small-scale ESN developed during the final stage of Phase I. The goal of the feasibility demonstration was to confirm that the ESN concept could be successfully realized through the following R&D effort during Phase II. In fact, the small scale ESN system could be easily expanded into a system with a substantially increased number of EO sensors.

3. System configuration

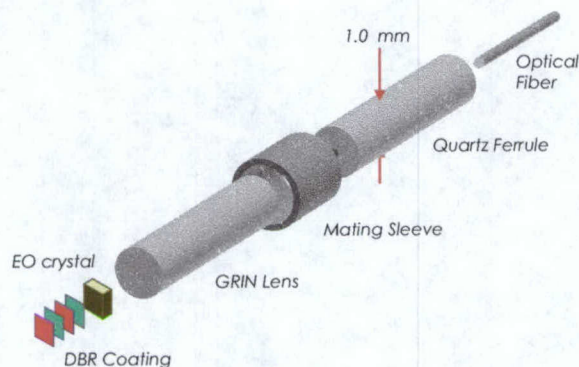


Figure 3. Fundamental configuration of the EO sensor.

The fundamental structure of the individual EO sensor units remains very similar to the EO probe used in the EO field-mapping system. As shown in Fig. 3, an optical fiber from one of the output ports of the device chosen for optical-beam distribution is guided into a quartz ferrule that provides ideal alignment of the fiber to a gradient index (GRIN) lens. The GRIN lens then focuses the input beam into an EO crystal. On the opposite facet of the EO crystal, a distributed Bragg reflector (DBR) coating is deposited in order to maximize the returned beam power. Miniaturized GaAs tips have been used effectively as EO crystals for field detection. However, as this SBIR project progresses into Phase II, we will perform a comprehensive study on GaAs as a possible EO sensor for on-site array applications. In particular, effects such as significant temperature and moisture variations and the direct illumination of sun light on the GaAs EO probe will be the main focus of the study. Based on this investigation, if necessary, proper means for protecting the EO sensor unit will be devised. Furthermore, we will endeavor to find new EO materials that may have better performance and more stability than GaAs for potentially harsh ESN applications. These could include CdTe, ZnSe, or others.

In particular, Opteos will maintain close communication with MDA and the Georgia Tech Research Institute (GTRI), as they are in the best position to provide Opteos with expert advice on the operating parameters for typical field-deployed antenna arrays. Once Opteos receives practical parameters for representative environmental conditions, the existing EO sensor will be tested under such operating conditions to study how the stability of the EO sensor might be affected. Opteos expects to obtain practical conditions for such parameters as temperature, humidity, and level of daylight radiation ranges. In addition, detailed projections for mechanical requirements will also be considered during the EO-sensor stability test.

In order to test and develop the optical-signal-distribution unit, the existing EO mainframe for the field-mapping system (Fig. 4) is used as a temporary optical mainframe for the ESN. An optical mainframe specifically designed for the ESN application will be developed during Phase II. We anticipate that the mainframe for the eventual ESN system would include an integrated beam source in the form of a compact laser, likely fiber-based, and with a higher output power at a wavelength of 1064 nm. The integration of a compact laser source as a part of the mainframe

will have the greatest impact for making the ESN system one that is compact and mobile. With the existing optical processing unit used as the temporary mainframe during Phase I, the optical pulse-train from an external, phase-stabilized, mode-locked laser (100-fs-duration pulses; 80-MHz pulse repetition rate) is used as an optical beam source. The laser wavelength is tuned to 905 nm and the average input power to the fiber is attenuated to around 15 mW to avoid two-photon absorption by the GaAs sensor, the standard EO-probe material used by Opteos. For the EO-field-mapping application, an EO probe is directly attached to the mainframe through an optical fiber and an FC connector. However, for the ESN application, the optical signal distribution unit is placed between the mainframe and multiple EO sensors in order to provide proper signal distribution to the EO sensors.

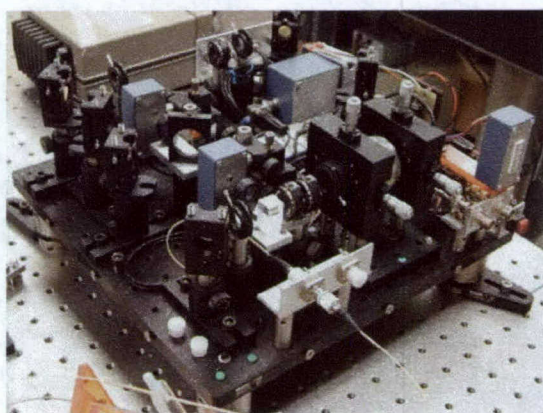


Figure 4. EO mainframe for the field-mapping system. This EO mainframe was used as a temporary mainframe for the ESN development during Phase I.

The optical mainframe plays a very critical role in the EO-sensor-network system, as it provides proper control of the laser beam properties and converts the optical signal to an electrical signal for display by the readout electronics. Figure 5 shows the schematic of the EO mainframe used during Phase I. The optical mainframe is designed based on the use of a 12 in. \times 12 in. optical breadboard as a platform (Fig. 5). Two mirrors are to be used at the beam input port in order to eliminate any spatial variation of the input beam (i.e., a laser beam can be directed along any path desired by using two mirrors in series). The vertically polarized input beam will then travel through an optical isolator and a $\lambda/2$ wave plate, where destabilizing reflections back into the laser can be quenched, and the polarization of the beam is changed into the horizontal direction. The reference signal generation unit will consist of a second photodetector and associated electronics. A part of the input beam is directed into the photodetector B by a non-polarization-dependent beam splitter. The photodetector B can convert the optical pulse train into an electrical signal, and this electrical signal will be converted into a sinusoidal reference signal by a straightforward electronic circuit. For the work in this Phase I grant, we have used a Ti:sapphire laser with an 80-MHz pulse repetition rate as the optical source for the system, and we generated a 10-MHz reference signal from the reference signal generation unit.

A polarization-dependant beam splitter that is oriented to transmit the horizontal polarization allows the beam to be passed on to the polarization control unit, which is a cascade of one $\lambda/4$ waveplate and one $\lambda/2$ waveplate. This polarization control unit will provide both quarter-wave and half-wave retardation to the input beam. The quarter-wave retarder can generate an elliptically polarized beam from a horizontally polarized input beam, and the half-wave retarder offers arbitrary control of the elliptically polarized beam in terms of polarization axis rotation. As a result, we can adjust the position of the half-wave retarder so that the polarization axis of the beam would be perfectly aligned to the c-axis of an attached electro-optic sensor.

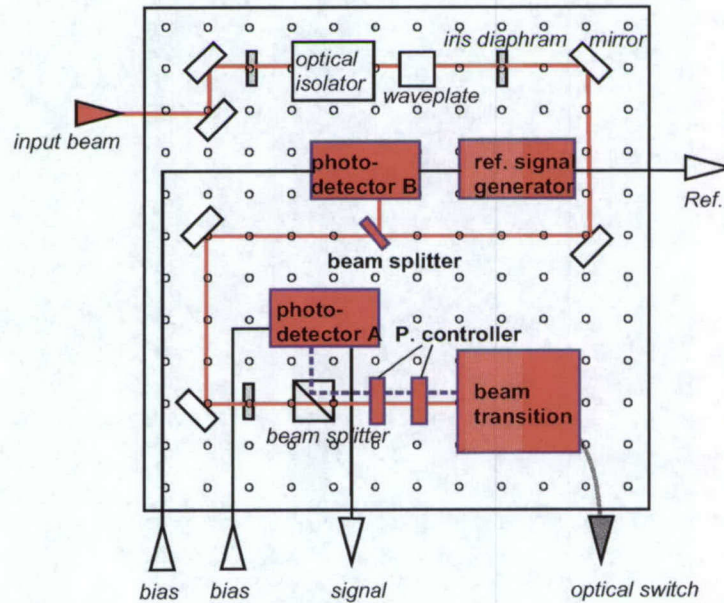


Figure 5. Simplified layouts of the optical mainframe used during the Phase I SBIR project. Red solid lines represent input beam path while blue dashed line represent the return beam from the probe, respectively.

The reflected beam from the EO sensor, containing the electric field information due to the birefringence and presence of the microwave field inside the crystal, travels back through the half- and quarter-wave retarders again. Since the beam passes the half-wave retarder twice (as an input beam and return beam), the resultant contribution of the half-wave retarder is nullified (full-wave retardation). However, the quarter-wave retarder now offers a half-wave retardation to the beam since the beam passes the retarder twice. By choosing the proper position of the quarter-wave retarder, we can obtain a linearly polarized beam with a 45-degree angle from the horizontal axis. Even though the beam regains its linear polarization, it will still contain the EO information at a small angle to the polarization axis. Thus, about half the power of the reflected beam will be routed to a photodiode, since the beam is no longer horizontally polarized. Finally, the photodetector A converts the optical EO signal into an electrical signal.

The beam-splitter to photodetector B is a partially metal-coated glass substrate that diverts 10-20% of the incident light for generating a periodic electrical signal at the frequency of the pulse-repetition rate of the laser being used. The in-house-built Reference Signal Generator then digitizes this electrical signal, which has a phase that is locked to that of the laser, and makes it available for use as a synchronization signal for the synthesizer that serves as the source to the device under test. The actual system of Fig. 5 can be seen in the photograph of Fig. 4. In practice, a free-space beam of 150-fs-duration pulses from a Ti:sapphire laser tuned to 905 nm is directed into the optical mainframe.

As shown in Fig. 6, the optical mainframe was placed between the pulsed laser source and some number of EO sensors, depicted here as four. The optical mainframe controls the input laser beam so that the beam can successfully detect the electric field at the EO sensors. Also, the return beam from the EO sensors, containing the EO signal, can be processed within the optical mainframe in order to convert the optical EO signal into an electrical signal that can be read by low-frequency instruments.

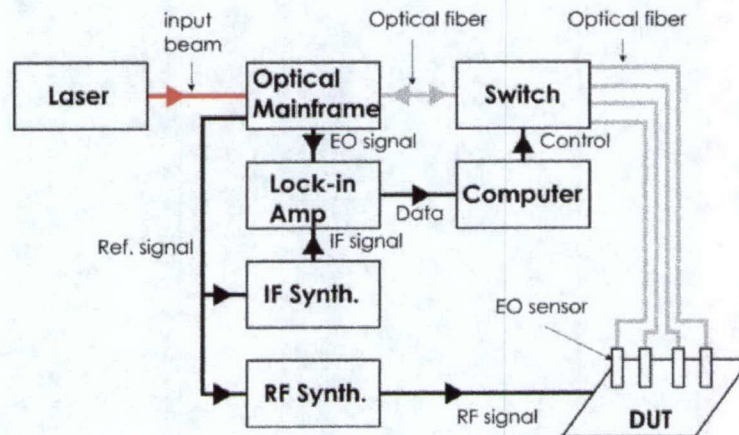


Figure 6. Schematic of entire EO sensor network system based on four EO sensor units.

In the small scale ESN system (Fig. 6), we use a lock-in amplifier as the readout instrument, making it possible to interpret both the amplitude and phase of the microwave signal simultaneously. However, we expect that different type of instruments can also be used for the readout instead of the lock-in amplifier (e.g., a spectrum analyzer), if it is necessary. Also, in addition to directing the EO signal toward the lock-in amplifier, the optical mainframe has the capability to generate a system-wide common reference signal. By using this reference signal, all the electronics in the system can be synchronized to the pulse train of the input pulsed laser beam, and as a consequence, it is possible to simultaneously measure phase along with the amplitude of the electric field from the DUT. As mentioned earlier, the optical mainframe shown in Fig. 4 and 5 was used as a temporary optical mainframe during Phase I of this SBIR project. During the following second phase, a designated optical mainframe with an integrated, compact laser source will be developed and used for the EO sensor network system.

4. Four channel optical switch

The optical switch distributes the input laser beam from the optical mainframe to individual EO sensors in a sequential fashion. At the same time, the return beam containing the EO signal can be directed back to the optical mainframe via the optical switch. Since the polarization difference between the input and output beam is to be detected as an EO signal, it is very important that the optical switch maintains the polarization of the beam during these transitions. Also, it is desirable to have only a small optical loss in the switch so that as much of the EO signal as possible from the probe can be transferred to the optical mainframe. Finally, a switch with a shorter switching time is desirable in order to reduce the sweep time of the sensor network, particularly when there are a large number of probes in the EO sensor network.

For the purposes of the feasibility study, we have decided to use a 1×4 optical switch – one input to four outputs. Through a search for commercially available optical switches, we have been able to identify three manufacturers that have a capability of manufacturing an optical switch for the EO sensor network application. All three manufacturers provide standard devices at the common telecommunications wavelengths of 1.3 and 1.5 μm . At our desired wavelength of 900 nm (for the Phase I), they only produce customized optical switches upon request. Among these manufacturers, two can build an optical switch with very fast switching times (~ 10 ns). However, after receiving quotations from those manufacturers, we determined that the costs for those fast switches is prohibitive for this Phase I project, especially considering that we wish mainly to prove feasibility. In contrast, one company (LIGHTech Fiber optics, Inc.) has provided a very reasonable quotation for an optical switch with a longer switching speed (10 ms). Thus, even though switches with better performance in terms of switching speed do exist, we decided to use the 10-ms component for the Phase I research, since it can provide very similar performance specifications as other switches for all properties except switching time. The key specifications of the optical switch that was utilized are listed in Table. 1.

Parameter	Value
Model number	LT 500 1 \times 4 SM
Switch control	TTL
Operating wavelength	905 nm
Insertion loss	2.0 dB typ \sim 3.0 dB max
Switching speed	10 ms typ. \sim 15ms max
Repeatability	$< \pm 0.02$ dB
Crosstalk	< -70 dB
Back reflection	< -55 dB
Fiber	3M 4224
Connector	FC/APC
Physical size	14 mm \times 50 mm \times 70 mm

Table 1. Key parameters of LIGHTech optical switch.

The switch package, shown in Fig. 7, is fitted with a 14-pin header, to which power is supplied at +5 V levels for TTL control of the optomechanical switching mechanism. We have specified 3M single-mode fiber (model # 4224) to match the mode size of the single-mode fiber we use within the EO mainframe and to guide the laser beams to the probes. Each input and output fiber is terminated in an FC fiber-optic connector.



Figure 7. Lightech LT500 1x4 fiberoptic switch. The single input port and the 4 output ports are fitted with 3M single mode fiber, model 4224, with an approximate 5- μ m-diameter mode profile within the guide.

5. Design of optical switch control circuit

Review of our immediate needs for this fiber-optic switch led us to decide that the control parameters should include: 1) being able to manually switch the fiber channel via a four-pole selector switch, 2) having a means by which to determine which channel has been selected, and 3) knowing when the fiber switch has run into an error and being able to reset it. These needs were constrained by the timing diagram provided by the manufacturer, which dictated that a "strobe" pulse must be used to tell the fiberoptic switch to read its data lines to determine when a channel is to be activated. This pulse must be greater than 60 ns in length, and valid information must be present on the data lines for 10 μ s after the strobe pulse has been pulled to a low logic level. After this, the fiberoptic switch enters a busy state that will last less than 60 ms before it either returns to a ready state or enters an error state.

The simplest and most convenient method to design the control circuitry for the fiberoptic switch involved using a basic synchronous sequential logic system. In this type of system, combinational logic, which consists of simple logic gates, is augmented by a memory device that is typically controlled by a clock-pulse generator. The design chosen here implemented a basic 555 timer chip to generate clock pulses of approximately 800 ns length and a period of 1.46 μ s, much longer than the 60 ns specified, but also much shorter than the listed 10 ms switching speed. This corresponds to a frequency of nearly 700 kHz, which is outside of the normal operating range of the typical 555 timer. Fortunately, this particular timer chip ran smoothly, but a more appropriate crystal oscillator should be considered in the future. These clock pulses governed two flip-flops, which are used to send the reset and/or strobe pulse to the fiberoptic switch when selected via a momentary two-pole switch. Two OR gates served as a two bit encoder from the four-pole channel-selector knob, and the output of this encoder provided the data lines to the fiber-optic switch. The 10 μ s data time is satisfied since the four-position selector knob is constantly providing information to the data lines.

[illegible]

Future design considerations for this control circuitry range from minor upgrade to major overhaul. The issue of most concern at present is that there is no method to guarantee which channel is selected when the system is first powered on. A simple "power-on reset" circuit can be implemented at minimal cost to solve this need and guarantee that the fiber-optic switch

always starts itself on channel 0. The next issue is that holding the momentary switch in the strobe position will send continuous pulses to the fiber-optic switch telling it to change channels whenever it returns to a ready state. This could be solved by redesigning the logic to follow an algorithmic state-machine format. However, it seems more likely that the future should involve automated computer control instead of a manual switch. In this case, the logic circuitry would be discarded for a more sophisticated and flexible interface with a computer. At its simplest, a parallel port interface could be used to transfer data to the fiber-optic controller from some software program such as LabView. Parallel ports are limited, though, by high cable costs, lack of available ports on many computers, and short cable lengths. Alternatively, a serial port connection could be used in conjunction with a microcontroller or possibly just a UART (Universal Asynchronous Receiver/Transmitter) chip. This would require a greater investment in time for design work and programming, but would allow for much greater flexibility in terms of distances and interfacing. Figure 8 shows the schematic diagram of the optical-switch-control circuit used to manage the 1×4 optical switch manufactured by LIGHTech Fiberoptics, Inc.

Figure 9 shows the test control circuit assembled on breadboard. The picture also shows the optical switch on lower left hand corner. The control circuit required single DC bias at +5V for its operation, and optical channel can be manually selected in sequential manner by pushing a pushbutton switch in the circuit. Even though we expect to use an optical switch with substantially increased number of channels with higher switching speed during the Phase II, the fundamental configuration of this control circuit could be used to for larger scale ESN during the Phase II. Also, the control circuit to be developed during the Phase II will be fully computer-controlled so that the selection of an optical channel and data acquisition can be managed by a single computer.

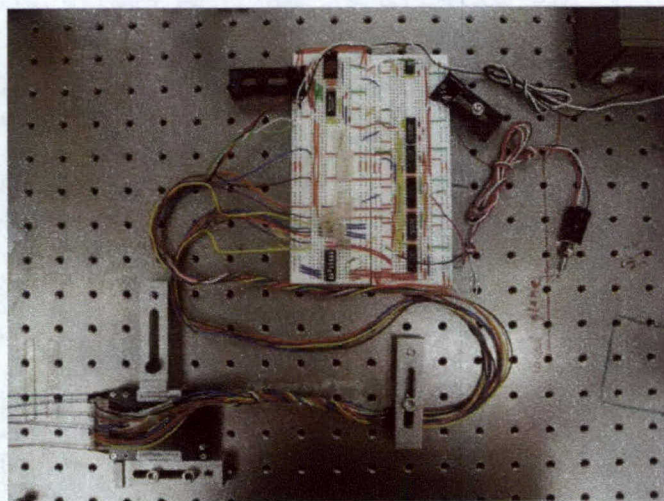


Figure 9. Optical switch (bottom left) and its controller circuit. The controller circuit is assembled on a simple breadboard for testing.

6. Performance evaluation of optical switch

It was expected that we should have been able to most easily acquire identical signals from the probes attached to each channel of the fiber-optic switch if each of these channels had tight tolerances with respect to insertion loss. An inspection certificate was included with the switch listing the insertion loss for each channel. Typical values for the channels are 2.0 dB, with a 3.0 dB maximum. Verification of these values was necessary to ensure that we understood any changes in the operation of the ESN system.

Optical Port	Insertion Loss (dB)
Ch. 0	2.30
Ch. 1	2.27
Ch. 2	2.56
Ch. 3	2.01

Table 2. Insertion losses provided by LIGHTech for the fiber-optic switch

Utilizing the optical mainframe described earlier, we easily compared output-beam powers destined for the probe by using a fiber-optic power meter at the end of a short fiber patch-cable attached to the FC connector at the output of the optical mainframe. After the beam-power measurement with the patch cable, this section was replaced by the optical switch, and loss from individual channels was measured separately. Ideally, this method provides for removing the effect of losses due to the FC-to-FC connection point, since both the patch cord and the switch suffer from the same effect. However, in reality, we have seen that the FC-to-FC connection can cause losses that vary between 0.25 dB and 1.5 dB. These variations are most likely caused by dirt and dust particles that randomly adhere to the tip of the FC connector, as it appears these can be removed by a cleaning process.

Optical Port	Optical Power (mW)	Insertion Loss (dB)
Patch cable	17.2	--
Ch. 0	7.90	3.38
Ch. 1	6.70	4.09
Ch. 2	6.25	4.40
Ch. 3	5.85	4.68

Table 3. Measured insertion loss of the fiber-optic switch

The measured values appear to show a great degree of deviation from those shown in the inspection certificate. However, assuming a rigorous FC connector cleaning routine to minimize losses at the connectors, a loss profile comparable to the expected value is likely attainable.

In addition to the loss characteristics, it was important that individual channels of the optical switch have stable, or ideally, identical polarization characteristics, since the EO-field-sensing technique relies on the detection of beam-polarization variations to obtain the amplitude and

phase of the microwave electric field. As a result, the electro-optic field-mapping system was constrained by the need for consistency between these ports to be able to accurately compare amplitude and phase information from the separate probes. A simple polarization test was useful to establish the response of each channel.

One difficulty in using a fiber-optic system that relies upon polarization states to determine measurement values is that optical fiber is susceptible to changes in birefringence when subjected to bending and twisting. These changes cause the polarization state of the light traveling through the fiber to change. Because of this effect, we may find the polarization state is no longer ideally linear due to the patch cable that lies between the fiber coupler and the fiber switch. Of course, this effect will be constant for all four channels, and correspondingly the input fiber may have a similar constant effect. However, the current meter-long length of each output channel fiber may respond in a unique manner to its resting position.

A typical polarization measurement setup allowed convenient characterization of the polarization state of an optical beam. Figure 10 shows our simple test using a brace to support the FC connector for each output fiber followed by a lens to collimate the output beam and then an optical polarizer, acting as the analyzer, and power meter. If the output beam has ideal linear polarization, a maximum and minimum output power would be observed while rotating the polarizer, and the minimum power would be near zero if the axis of the polarizer was set to be perpendicular to the polarization of the incoming beam. If the beam has elliptical polarization, one can still observe alternating maximum and minimum beam power while rotating the polarization. However, in this case, the ratio between the maximum and minimum beam powers would become much lower. In the other extreme from linear polarization, if the beam is circularly polarized, the power reading should remain unchanged regardless of the polarizer setting.

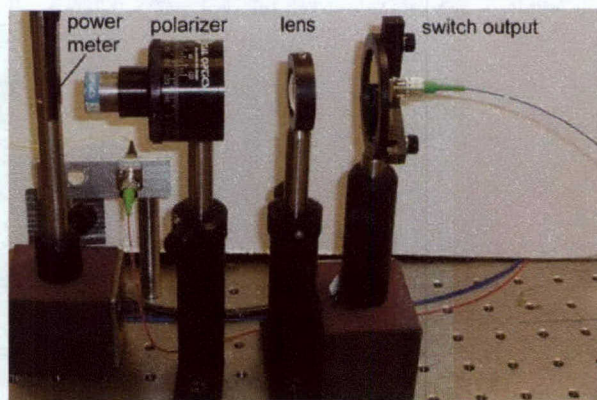


Figure 10. Beam polarization test setup for the optical switch. The output beam from the selected channel of the optical switch is focused into the polarizer and the beam power is measured by the power-meter head on the far left.

Assuming no changes throughout the various fibers and the fiber switch, the power meter would respond to an ideal linear laser beam by showing zero power when the analyzer is set at 90° and 270° while showing maximum power at 0° and 180° , or vice versa. Table 4 shows the actual measured values.

Channel	Output Power (mW) vs Polarizer Angles			
	0°	90°	180°	270°
0	5.3	2.3	5.1	2.4
1	5.0	1.9	4.6	1.8
2	5.9	0.3	5.6	0.2
3	0.9	5.0	0.5	5.1

Table 4. Polarization states via cardinal angle power measurement

The results in Table 4 clearly indicate that the polarization state of the beam leaving the optical mainframe is changing to a somewhat elliptical state after passing through the various fibers and the switch itself. This result is not ideal, especially since the change is not consistent between all four channels. However, it was instructive to check if adjusting the quarter- and half-waveplate in the optical mainframe could lead to a linear polarization at the output port of the optical switch. As shown in Table 5, it was possible to compensate the effects of birefringence in the various optical fibers of this system. The small power shown at 270° was likely due to an optical path that was not perfectly centered and orthogonal to the plane of the polarizer.

Later, we adjusted two wave plates mounted in front of the fiber coupler in the optical mainframe (Fig. 5) in order to achieve uniform performance from the individual output channels. Noticeable in this case is that the birefringent properties of our chosen single-mode optical fiber are such that twisting and bending strains cause the polarization state to change quite easily. This change suggests that in a multi-probe system, the lengths of fiber will need to be mounted in such a way as to prevent unexpected movement that might affect operation. A simple looping and twisting of the fiber similar to a fiber-based waveplate could be a sufficient means by which to calibrate each probe such that each channel would exhibit the same birefringence leading to agreement of amplitude and phase values at equivalent points in a given device under test.

Channel & Quarter and Half Waveplate Angle	Output Power (mW) vs Polarizer Angles			
	0°	90°	180°	270°
0 (110° , 20°)	6.6	0.0	6.3	0.6
1 (90° , 90°)	5.6	0.0	5.3	0.7
2 (80° , 40°)	5.3	0.0	5.0	0.6
3 (110° , 90°)	5.0	0.0	4.8	0.4

Table 5. Polarization states via cardinal angle power measurement after adjustment of optical mainframe waveplates.

Having examined the operating characteristics of the fiber-optic switch, we turned our attention to examining the possibility of attaining adequate and consistent electro-optic signals with the switch inserted at the output side of the optical mainframe. A control measurement was typically taken using a patch antenna whenever the optical mainframe was modified or enhanced.

This antenna, operating at 4.003 GHz with an input power of +18 dBm, was probed using the input laser source operating at 905 nm entering the optical mainframe at a strength of approximately 76 mW. These conditions yield a reflected signal from the probe of -8 dBm and an EO signal at the lock-in typically around -87 dBm, without the introduction of the optical switch. The location of this measurement point on the antenna is at the far end of the antenna opposite the input port and centered from both sides.

Channel	Quarter Waveplate	Half Waveplate	Reflected Power (dBm)
0	30°	330°	-16.43
1	135°	68°	-19.00
2	44°	54°	-17.00
3	186°	320°	-21.00

Table 6. Reflected power in EO Probe for 100 mW power into optical mainframe

At this part in the development of the optical mainframe it is prudent to keep in mind the balance of system performance versus the needed input power. Knowing that adding the fiber-optic switch would likely cause a halving of the previous optical power reaching the probe, it was necessary to decide the wisdom of potentially doubling the input power considering the trade-off in future plans for possible laser sources.

With 100mW chosen as a reasonable input power based on aforementioned considerations, and having tuned the optical mainframe to operate as efficiently as possible, Table 6 shows a major reduction in the reflected signal strength from the probe when the fiber-switch is inserted. This was a concern until it was realized that the electro-optic modulation signal was rather insensitive to the loss of power due to the presence of the switch (Table 7). These values suggest that despite the unequal losses measured earlier between the four channels, the optical power transmitted through the switch is still sufficient enough to maintain a consistency between these channels.

Channel	Quarter Waveplate	Half Waveplate	EO Signal Power (dBm)
0	240°	240°	-84.0
1	20°	338°	-84.0
2	172°	60°	-85.0
3	120°	10°	-87.5

Table 7. EO Signal from Probe for 100 mW power into optical mainframe

The ability of the field-mapping system to successfully and consistently measure the patch antenna over the four fiber-optic channels is an encouraging sign for the future of this project and suggests that the likelihood of reaching the goals set out in the technical objectives is high.

7. Fabrication of small scale ESN

Originally, the intention was to build a small-scale ESN with four EO sensors based on the use of the 1×4 optical switch. However, we a damaged output fiber was discovered on one of the optical-switch channels. Since the estimated repair time for the switch by the manufacturer was unacceptably long, we decided to build the small-scale ESN with three sensors rather than four. The overall configuration of the EO sensor was shown in Fig. 3. Miniaturized GaAs tips with distributed Bragg reflectors on one side were used as the EO-sensing material. The physical size of the tip was $400\text{ }\mu\text{m} \times 400\text{ }\mu\text{m} \times 200\text{ }\mu\text{m}$ and the reflection layer was designed to achieve more than 95 % beam reflection at 905-nm wavelength. The GaAs tip was attached to a gradient index (GRIN) lens, which tightly focused the incoming optical beam into the GaAs tip. A single-mode optical fiber was aligned and attached to the center of the GRIN lens using a quartz ferrule and a mating sleeve. Ultraviolet-light-curable optical cement was used for each connection point in the sensor. The other end of the optical fiber was terminated by an FC/APC optical connector, which allowed a convenient connection and disconnection of the sensor to the output port of the optical switch. Even though there is no specific limitation for the length of fiber, we maintained a length of 1 m for each individual EO sensor, mainly for the ease of handling.

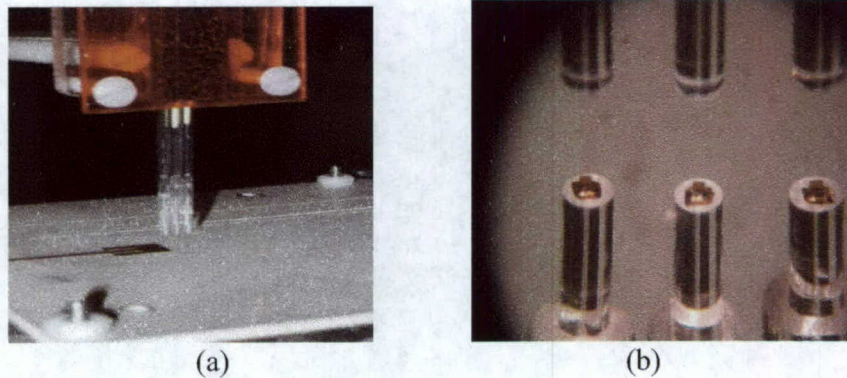


Figure 11. Three EO sensors linearly arranged in an array. (a) The EO array mounted on sensor holder, and (b) magnified view of the GaAs sensors mounted on the bottom of their respective GRIN lenses, where the image is reflected from a mirror below the probe assembly. The center-to-center spacing between the EO sensors is 2 mm.

After the completion of the probe assembly, the three EO sensors are mounted on sensor holders to form a linear array. For the practical application of the EO-sensor array, we expected that the spacing between the sensors would be mainly determined by the configuration of the antenna or array under test. The separation between the sensors (or total number of sensors) needs to be carefully selected so that one sweep of the EO array on an AUT could provide

sufficient information on the antenna elements. In general, one could expect that the EO linear array needs to have smaller spacing between the EO sensors in order to be used for antennas or arrays with higher operating frequency or finer electrical structures on them. During Phase I, we set the separation between the EO sensors to be 2 mm, which is equivalent to the wavelength of an EM wave with 150-GHz frequency in free space.

The optical switch control circuit shown in section 6 was designed to achieve convenient control of the 1x4 optical switch, particularly during the early test stages for the optical switch by allowing us to manually control the device. However, in order to control the optical switch during multi-dimensional scanning, where the computer performs position control and data acquisition, it was necessary that the computer control the optical switch along with other components in a synchronized manner. As an effort to accomplish two-dimensional scanning of multiple EO sensors, we decided to use a modified parallel-port connection directly to the control port of the switch.

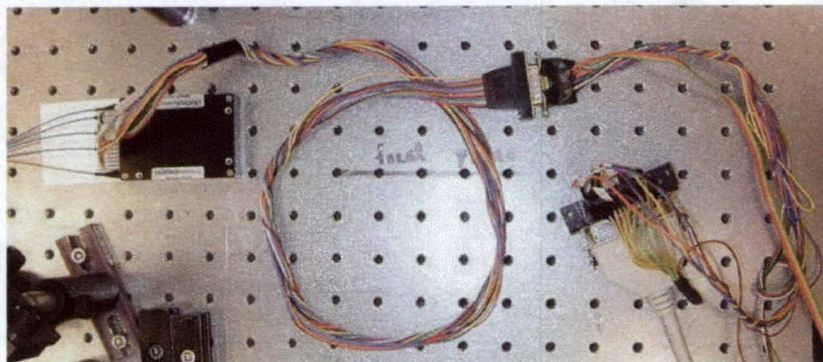


Figure 12. Optical Fiber Control Port

Table 8 details the standard PC parallel-port pinout. Shaded lines indicate which pins were chosen to control the 1x4 optical switch. In the current design, Data Bits 0 and 1 on the optical switch matched with D0 and D1 in the parallel port specification. That is, they used Centronics Pins 2 and 3, respectively. The Strobe line was controlled via D2 (Centronics Pin 4) and the Reset line was controlled via D3 (Centronics Pin 5). Also of importance were status indicators from the optical switch. The Error indicator was examined on PaperEnd (Centronics Pin 12) and the Ready/Busy indicator was monitored on Select (Centronics Pin 13).

Mating between the PC parallel port and the optical switch occurred via an intermediate connection using a DB15 connector to allow for easy changes in control between the manual logic-based selector and an automated computer system. Because this wiring was established for the manually controlled system before the decision to use a parallel port interface, there was a mismatch between the parallel port's standard DB15 pinout and the pin selection that was chosen. The optical-switch-to-DB15 cable pictured in Figure 12 is detailed in Table 9.

D-sub	Signal	Function	Source	Register	Register Bit #	Inverted at Connector?	Pin: Centronics
1	nStrobe	Strobe D0-D7	PC ¹	Control	0	Yes	1
2	D0	Data Bit 0	PC ²	Data	0	No	2
3	D1	Data Bit 1	PC ²	Data	1	No	3
4	D2	Data Bit 2	PC ²	Data	2	No	4
5	D3	Data Bit 3	PC ²	Data	3	No	5
6	D4	Data Bit 4	PC ²	Data	4	No	6
7	D5	Data Bit 5	PC ²	Data	5	No	7
8	D6	Data Bit 6	PC ²	Data	6	No	8
9	D7	Data Bit 7	PC ²	Data	7	No	9
10	nAck	Acknowledge	Printer	Status	6	No	10
11	Busy	Printer busy	Printer	Status	7	Yes	11
12	PaperEnd	Paper end, Empty	Printer	Status	5	No	12
13	Select	Printer Selected (online)	Printer	Status	4	No	13
14	nAutoLF	Generate automatic line feeds	PC ¹	Control	1	Yes	14
15	nError	Error	Printer	Status	3	No	32
16	nInit	Initialize Printer	PC ¹	Control	2	No	31
17	nSelectIN	Select Printer (place online)	PC ¹	Control	3	Yes	36
18	Gnd	Ground Return for nStrobe, D0					19,20
19	Gnd	Ground Return for D1, D2					21,22
20	Gnd	Ground Return for D3, D4					23,24
21	Gnd	Ground Return for D5, D6					25,26
22	Gnd	Ground Return for D7, nAck					27,28
23	Gnd	Ground Return for nSelectIN					33
24	Gnd	Ground Return for Busy					29
25	Gnd	Ground Return for Init					30
	Chassis	Chassis Ground					17
	NC	No connection					15,18,34
	NC	Signal Ground					16
	NC	+5V	Printer				35

¹Setting this bit high allows it to be used as an input ²Some Data ports are bidirectional

This chart is compiled from information provided via a picture available at

<http://zone.ni.com/devzone/conceptd.nsf/webmain/72C6FC6CE4AD4D1386256B1800794596?opendocument>

Table 8. PC Parallel Port pinout specificatio

It should be noted that the electrical current required for the optical switch prevented it from being powered through the parallel port. Consequently, an external 5-volt power supply was used. Also, only two data bits were necessary to completely address the four available channels on the optical switch. However, the switch would not operate properly unless all six of its data bits had a valid TTL level on them. For this reason, data bits two through five were permanently tied to ground.

In addition to the parallel port hardware, we have modified the two-dimensional scanning software, originally written for scanning with a single probe, so that the data acquisition from different sensors would be feasible while the position of the sensor arrays was continuously changing. Figure 14 shows a flow chart of the scanning software employed for multiple EO sensors. With a multiple probe configuration came the decision of how to properly manipulate the probe position to gather the required information from various devices under test. Two methods

were considered for this ESN. Both methods followed the same basic flow control, that being to take measurements from each of the individual probes in sequence at a given point before moving on to the next coordinate. The difference becomes apparent when the type of device under test is revealed.

The first method, diagrammed in figure 15, shows the group of probes moving from a row of devices to the next row of devices to take point measurements of individual elements of an array. Depending on the number of probes available, that many columns of elements can be scanned at each stop of the probe assembly. The software moves the assembly and then takes data for each probe by changing the channel of the optical switch. After each channel is selected and the signal measured, the probe assembly moves to the next group of elements. In this example, there are eight groups of three elements. The probe assembly makes eight stops and measures the three elements using the three probes at each stop.

Optical Switch Pin	Opteos' DB15 Conversion Cable	Pin Function	Parallel Port Centronics Pin
1	15	Switch Power (+5V, 200mA)	NC ¹
2	14	Switch Ground	NC ¹
3	7	Controller Ground (+5V, 200mA)	NC ¹
4	8	Controller Power	NC ¹
5	13	Strobe (switch input)	4
6	1	Ready/Busy (switch output)	13
7	9	Error (switch output)	12
8	5	Reset (switch input)	5
9	12	Data Bit 0	2
10	4	Data Bit 1	3
11	11	Data Bit 2	NC ²
12	3	Data Bit 3	NC ²
13	10	Data Bit 4	NC ²
14	2	Data Bit 5	NC ²

¹Power is supplied through an external power source
²These pins are tied to a common ground

Table 9. Optical Switch to Parallel Port pinout

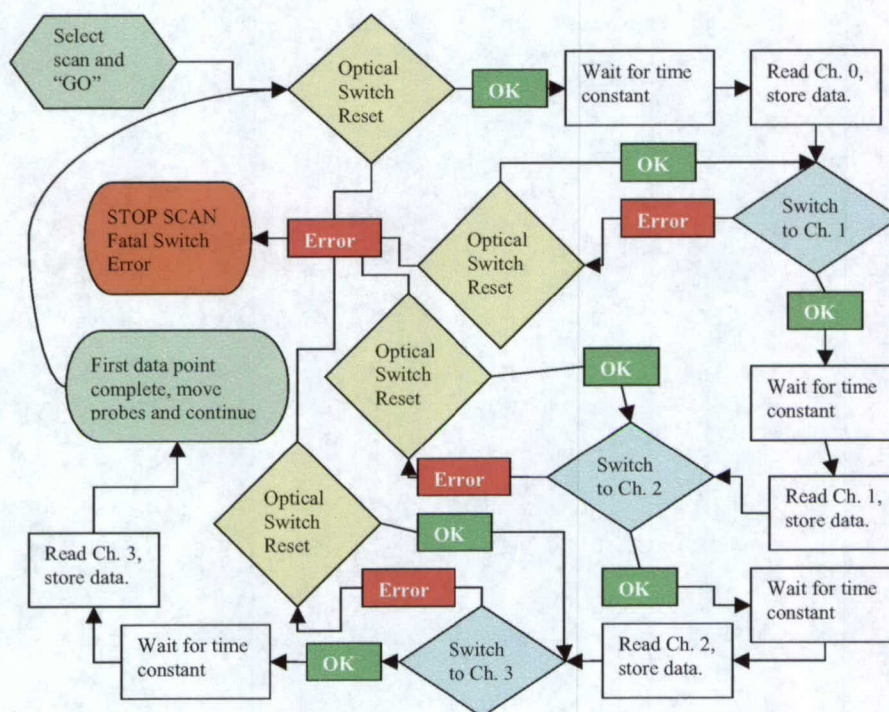


Figure 14. Software Basic Flow Control

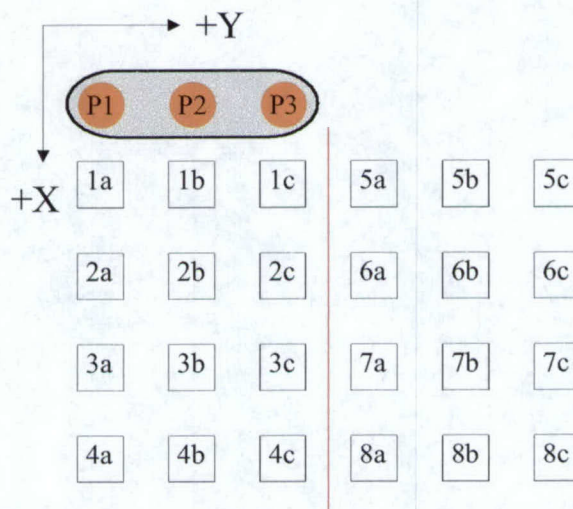


Figure 15. ESN Scanning sequence diagram.

The standard test method for Opteos' EO measurement system has been field-mapping of a 4.003 GHz patch antenna. To obtain an accurate set of data for this antenna, it is necessary to use a slightly different scanning method with the ESN as shown in Fig. 16.

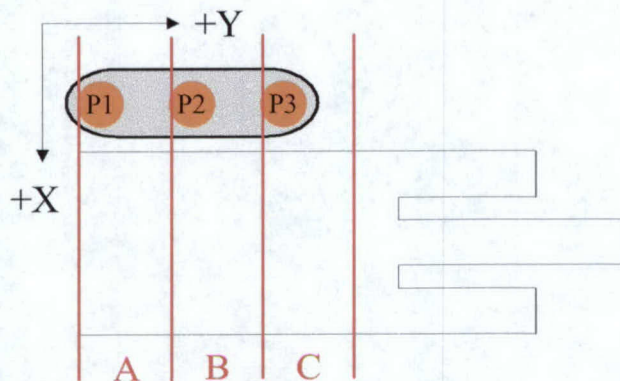


Figure 16. ESN Scanning sequence diagram for patch antenna.

Unlike the first method, where after scanning a number of elements along a column the probe assembly moves by a distance equal to the width of the probe assembly to scan the next column of elements, this patch antenna requires information of the radiating field as it exists between the individual probes. Because the probes are spaced with a 2 mm separation, this means that the second method will take much smaller steps in the y direction, with a maximum movement equaling the 2 mm spacing between the probes. Probe 1 will then have scanned over the entire area defined in Figure 16 as Area A. Likewise, Probe 2 will see Area B and so on. As before, at each movement in the x direction, the scanning software took data for all three probes. It then stitched together the three areas of data into one comprehensive field map. Again, the basic concept of modification to the scanning software was the same for these two methods. In each case, the software moved the probes, stopped to take data, and then moved on to the next location. With the ESN, each stopping point involved taking a measurement from each probe and then deciding how to store that data based on the makeup of the device under test.

8. Performance evaluation of the ESN

In order to evaluate the performance characteristic of the small-scale ESN system, we initially performed two-dimensional field scanning over the 4-GHz patch antenna by using only a single probe. The result of the single probe scan is shown in Fig. 17, and it is used as a reference to evaluate the scanning results obtained from the multi-probe ESN system.

The three EO sensors from the ESN system were placed on the same patch antenna and the scanning results obtained from the ESN probes are presented in Fig. 18. In this case, polarization control of the three probes was only available via the initial free-space waveplates in the EO mainframe. Since separate polarization control was not available for each of the three probes in the ESN, signal strength was maximized for one probe and the other two probes were left to operate in a non-optimized state. Comparing this scan to an earlier scan of the patch antenna using just one probe (Figure 17), it is possible to see that the amplitude and phase appear as

expected, although the signal is much noisier, resulting in the lower quality measurement that was observed.

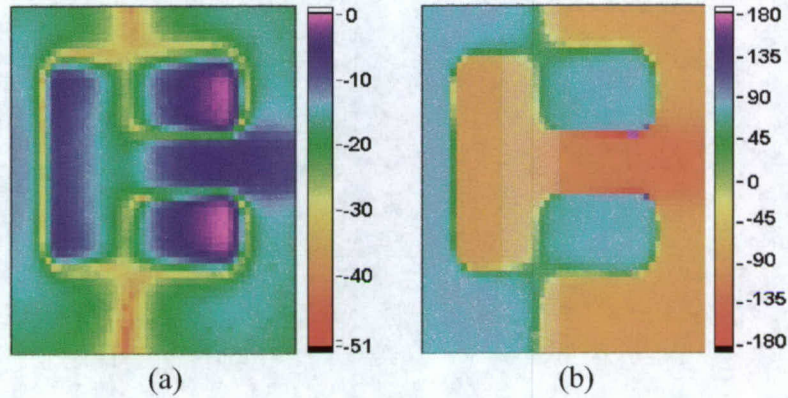


Figure 17. Field scanning results on the 4-GHz patch antenna by using a single EO probe. (a) Amplitude in dB and (b) phase in degree.

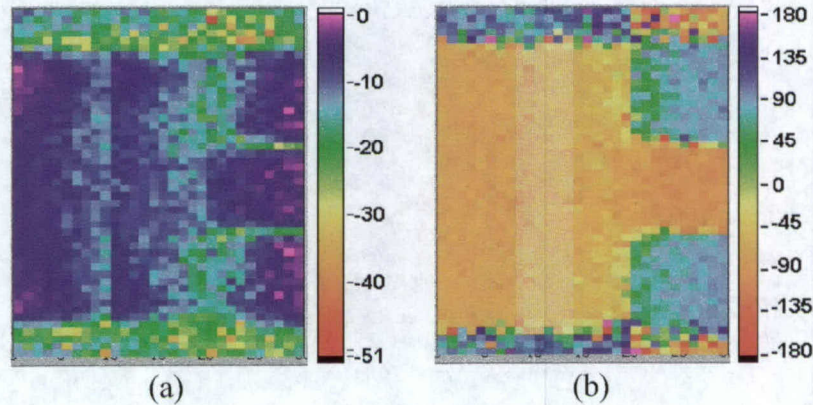


Figure 18. Field scanning results on the patch antenna by a three-sensor EO array without any calibration process. (a) Amplitude in dB and (b) phase in degree.

In addition to the low signal level, some visual discontinuities can be observed in the amplitude map, which indicates non-uniform response characteristics from each probe. This non-uniformity could originate from slightly different characteristics of the probe, or the non-uniform output characteristic of the switch could be a contributing factor for the overall non-uniform behavior of ESN system. There are two main factors that most likely determine the response characteristic of EO sensors – the optical beam power to the EO sensor and the polarization status of the beam. Based on the assumption that the high reflection coatings on the bottoms of the EO sensors have uniform performance, which is quite possibly true since the EO sensor tips were simultaneously fabricated in a batch process, then the amount of the beam that actually travels into the EO probe could decide the power of the reflected beam containing the EO signal information. As a result, a probe receiving an optical beam with a higher power may display a stronger EO signal than other probes under identical conditions. The other issue is the

polarization of the beam. It was discussed previously that the EO signal from the probe is encrypted into the polarization of the beam, and the difference in polarizations of input and return beams would determine the strengths of the EO signals. As a result, even though two EO probes are receiving optical beams with identical power, it is still possible to read different EO signals from them if one probe picks up additional birefringence along its beam path. Again, non-uniformities in these two factors – beam power and polarization – can be caused by the EO sensor or the optical switch. Based on various experimental setups, we were able to identify that the EO sensors have very uniform characteristics, and most of the non-uniformities in the ESN system originated from the optical switch.

The non-uniform polarization characteristics between EO sensors can be effectively canceled by adjusting the polarization optical components in front of the fiber coupler with respect to the selected output channel. However, it is unrealistic to manually adjust the polarization optics during scanning when a computer controls the movement of the probes and data are acquired automatically from the three probes. One alternative would be to install a fixed amount of polarization birefringence into each channel so that the overall polarization characteristics from each EO sensor could be uniform. This could be easily achieved by creating small loops of fiber with specific diameters, known as Lefèvre loops. By adjusting the orientation of the loops in each channel, the uniform polarization across all the EO sensors should be obtained. During the experiment, Lefèvre loops were inserted into the second and third probes in the ESN, making the polarization characteristics of those probes identical to the first probe. This allowed for the first probe to be optimized using the EO mainframe's waveplates, as usual, and then for the additional probes to be optimized afterwards with the loops. The optical switch introduced polarization changes that varied between its individual channels, and which were compensated for by the Lefèvre loops. An approximately 9-dB increase in overall signal strength was noticed during this measurement, which is significant in the resulting field map. Eventually, Opteos plans to replace the manually controlled polarization components with an in-fiber, computer controlled polarization controller. Thus, the polarization controller can be adequately adjusted with respect to the selected channel to compensate channel-to-channel polarization differences.

One aspect of the optical switch that still can cause non-uniformity in the measured signals between the individual probes is the differing insertion loss among the channels of the optical switch, which eventually leads to non-uniform beam power to the probes. These different loss values don't necessarily affect the resulting EO signal when the laser power to the whole system is strong enough to provide the required minimum optical power to each GaAs tip. However, because the new EO mainframe has elements that consume more of the currently available laser energy, it is likely that the probes were operating near their minimum threshold during the ESN tests. The normal method by which the minimum operating level is confirmed is the back reflection measurement. Table 6 shows back reflection measurements of a single probe for each of the four channels of the optical switch. During the ESN measurements, with increased laser power into the system, the three usable optical switch lines were all showing the same back reflection of -6.5 dBm, regardless of which EO probe was attached. It was likely that the large measured reflection here came from the optical switch itself, making it difficult to determine how much power reached the GaAs tip at each probe. A less precise method of evaluating the power reaching the probe tip is to measure the power of the laser light that is transmitted through the last optical stage before the probe fiber (after the optical switch in this case.) Table 10 shows

these values for the 1x4 optical switch. In measurements taken before the inclusion of the optical switch, values of 17 mW to 20 mW were common for proper operation of the EO probe. In the table, it should be noted that channel 1 of the optical switch is the damaged output, and as a result, only three output channels – channel 0, 2, and 3 – have been characterized. Currently, 15 mW to 20 mW is available to the three probes with 77 mW incident on the fiber coupler in the EO mainframe. (See Table 10) While these values were reasonable in the past, they do not take into consideration the additional return losses as the reflected signal propagates back through the optical switch and into the mainframe to the photodetector. A couple of dB extra loss at each additional fiber optic interface between the probe and the mainframe is significant.

Optical Switch Channel	Power Output (mW)
3	15
2	16
0	20

Table 10. Optical Switch output power (77 mW input to fiber coupler). Note that channel 1 could not be used due to mechanical damage.

To examine this operating condition in closer detail, each of the three probes used in the ESN experiment was connected to each line of the optical switch and a measurement was then taken at a reference point on the patch antenna that provided the largest available radiating field with the standard 4.003 GHz, 18 dBm input. Table 11 shows the EO signal that was measured. The results of each probe on line 3 agree with the results of each probe on its own line, whereas the results of each probe on line 2 and line 0 are similar. What is certain from the table is that line 0, with the largest power output, is likely to have a higher measured signal than the other lines. To confirm the hypothesis that signal variation was due to power requirements, an examination of EO signal strength of each probe on its appropriate optical switch channel was needed, with each channel providing the same optical power to its corresponding probe.

Optical Switch Channel	EO Probe Number	EO signal (dBm)
3	3	-91.8
2	2	-91.5
0	0	-88.2
3	3	-92.0
3	2	-90.5
3	0	-89.3
2	3	-89.7
2	2	-89.0
2	0	-90.5
0	3	-86
0	2	-86.5
0	0	-87.3

Table 11. EO signal from various channels (77 mW input to fiber coupler). Note that channel 1 could not be used due to mechanical damage.

Table 12 shows that when each channel is delivering 15 mW, by adjusting the beam power into the ESN with respect to the selected optical switch channel, the EO signals became more uniform. The result indicate that, if we can compensate the non-uniform beam power delivery to the probes, along with adequate polarization compensation, it is possible to calibrate the ESN sensors very accurately. Additionally, Table 12 shows the result of removing the 1x4 optical switch altogether and measuring the EO signal of each probe at a more normal power level of 20 mW. These two data sets confirm that having a common power input to the probes will provide more uniform results.

Optical Switch Channel	EO signal (dBm)
3	-87.1
2	-87.7
0	-86.2

Table 12. EO Signal for 15 mW output at each channel

Optical Switch Channel	EO signal (dBm)
3	-83.0
2	-83.0
0	-83.0

Table 13. EO Signal for 20 mW output at each channel (switch removed)

Under ideal circumstance, the use of an optical switch with uniform output characteristic over entire channel would be desirable. However, it is practical to expect a certain degree of non-uniformity from any commercially available optical switches. This can be calibrated by adjusting the input beam power to the optical switch with respect to the selected channel based on a pre-acquired characteristic of the channel. This method may require the use of a computer-controlled attenuator, which may increase the complexity of the ESN system. As an alternative, this power non-uniformity can be easily dealt with post-processing software. Since the power (or loss for a fixed input power) behavior of individual channels is a unique characteristic of the switch, we can create a fixed calibration matrix. The matrix can be applied to the measured data to compensate non-uniform power factor in the data.

Finally, Fig. 19 shows field maps obtained by three EO probes after adequate polarization and amplitude calibrations. The uniform polarization condition to the EO sensors was obtained by Lefèvre loops, and amplitude calibration was performed on the measured data based on the results shown in Table 12. As displayed in Fig. 19, the mapping results after proper calibration exhibit excellent agreement with the scanning results obtained by the single probe.

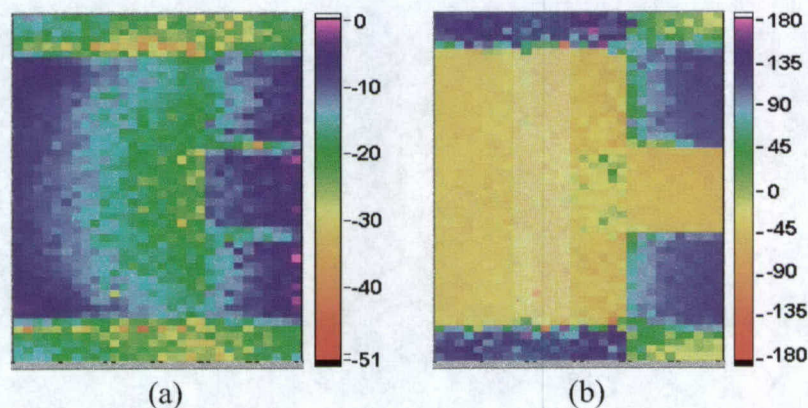


Figure 19. Field scanning results on the patch antenna by a three-sensor EO array with beam polarization and amplitude calibration processes. (a) Amplitude in dB and (b) phase in degree.

9. Phase II R&D plan

The primary objective of the Phase II MDA SBIR contract to be executed by Opteos will be the fabrication, test, and performance demonstration of a prototype linear electro-optic (EO) sensor array system to be used for the characterization and calibration of arrays of antenna elements. As such, it is expected that this network of sensors would be appropriate for rapidly conducting performance verification and troubleshooting measurements on arrays of radiating elements, including those that comprise modular panels that themselves may be combined to form a large phased-array radar. An additional goal of this SBIR program is to investigate the utilization of a compact, fiber-based laser source with a compact optical network in order to allow

measurements to be performed outside of the Opteos facilities, such as at the site of the radar-panel development.

Specific technical objectives of the Phase II SBIR program will include

- Expansion of the small-scale electro-optic sensor array developed during Phase I so that the prototype linear sensor array produced at the end of Phase II can cover a large number of radiating elements within an 18" \times 44" antenna-array panel.
- Investigation of the effects that environment and dispersion may have on the long sections of optical fiber used to couple the optical-beam analysis components to the EO sensors
- Design and development of a compact, mobile, optical mainframe through integration of a high power, fiber-based, pulsed-laser source into the optical processing unit
- Redesign and fabrication of new optical signal distribution infrastructure through the use of faster and more efficient optical switches.
- Development of data acquisition and optical-channel-control software.
- Investigation of the most effective means for calibrating individual sensor channels to produce a uniform response across the linear sensor array.

Compared to the feasibility demonstration performed during Phase I, a prototype ESN system produced at the end of this SBIR project would have a substantially increased number of EO sensors. During this SBIR, Opteos will use a linear arrangement of EO sensors in the primary design, as shown in Fig. 2. During the Phase II, Opteos will assume that the physical dimensions of the primary array under test are 18" \times 44", as suggested by the Georgia Tech Research Institute (GTRI). In addition to the physical size of the array, the operating frequency of the array under test, which will be taken to be in X-band, will be a strong consideration in the design of the sensor array dimensions and other properties. For example, since the spacing between the EO sensors will be a half-wavelength at the operating frequency, it is thus approximated that 30 to 40 EO sensors may be required to form the EO sensor array for the given specification.

With an increased number of EO sensors, it is critical to employ a high-performance optical switch with sufficient output channels, or multiple switches with a smaller number of output channels, or even a combination of optical switches and power dividers to form the required network. Fortunately, numerous optical switches and dividers with large numbers of output channels are commercially available, and Opteos will use such optical devices to form the ESN system. In addition, the speed with which one antenna array is evaluated will depend on whether each ESN element is addressed sequentially, or whether some can be interrogated in parallel. Another consideration may be whether the linear array is scanned in only one direction, or if there may be an advantage to using a series of, for example, two one-dimensional scans with a shift of sensors in the orthogonal, transverse plane in between.

In addition to the large number of EO sensors, Opteos will design and develop a new EO-mainframe, optical processing unit for the prototype ESN system during this Phase II. The proprietary EO field-mapping system that served as the predecessor of this ESN system utilized as its beam source a Ti:sapphire laser system pumped by a solid-state, cw laser that, in turn, was pumped by a diode-laser. Due to the large physical dimension of this laser system, it is difficult

and expensive to move the EO field-mapping system between laboratories and other test sites. This weakness of the EO field-mapping system must be addressed within the ESN system, since it is anticipated that the ESN system will need to be transported to locations where an array containing sensitive technology is located. We have identified that the use of a compact laser source for the ESN system would be the most important and immediate solution to achieve the required mobility for the ESN system. As a result of the Phase I effort to survey commercially available compact laser sources, Opteos has identified a fiber-based laser with specifications that satisfy all the requirements of the ESN application, once the manufacturer completes development of an RF phase-locking mechanism. With the use of this compact laser source, the ESN mainframe would have significantly smaller physical size than the mainframe used in the EO field-mapping system, making the ESN system mobile enough to be easily relocated. Not only should the fiber-based laser require less maintenance than the Ti:sapphire laser, but the cost of the fiber-based laser is approximately 50 to 60 % less than that of the Ti:sapphire laser, leading to a significant cost reduction for the complete ESN system. The mainframe will be modified to accommodate an integrated short-pulse fiber laser, as well as the different wavelength, 1.05 μm , that the new laser source will emit.

Since the fiber lengths between the optical-processing mainframe unit and the EO sensors may be somewhat longer, and may experience somewhat different environmental conditions, than those used in the R&D laboratory, Opteos will also investigate the effects that temperature, moisture, EMI, and ambient light will have on the fiber. One would typically expect that only temperature and mechanical stress would impact the inherent birefringence or possible the attenuation of the fibers, but a variety of harsh conditions will be imposed to evaluate the need to protect the fiber and maintain its mechanical and optical integrity.

In addition to the completion of the linear EO sensor array and new mainframe hardware, Opteos will investigate means to accurately perform an initial calibration of the ESN system. Since a large number of EO sensors will be used within the ESN system, it is very important to develop a systematic effective calibration process in order to achieve uniform responsivity characteristics over all the sensor elements. Opteos is planning to use a reliable RF structure (such as a simple antenna at the desired operating frequency) to generate a calibration table containing amplitude and phase response characteristics from individual EO sensors by placing them at identical positions on the antenna. Later, this table can be automatically applied to actual measurement data through the system software. This software will be presented through an intuitive, graphical interface that controls the positioning of the ESN array, the scanning, the data acquisition and manipulation, and the quasi-real-time display of the unit-cells' amplitude and phase information.



SBIR PROJECT

PHASE II PLAN

Embedded Electro-Optic Sensor Network for the On-Site Calibration and Real-Time Performance Monitoring of Large-Scale Phased Arrays

Contractor: Opteos, Inc.

Principal Investigator: Dr. John F. Whitaker

(734) 763-1324, whitaker@umich.edu

Contract Number: HQ0006-05-C-7155

Phase I Period: 03/07/2005 – 09/07/2005

Technical Monitor: Robert C. Parks

1. Phase I Technical Objectives

The Phase I SBIR project entitled "Embedded Electro-Optic Sensor Network for the On-Site Calibration and Real-Time Performance Monitoring of Large-Scale Phased Arrays" is corresponding to the MDA SBIR topic "Radar Systems Technology Innovative Concept", topic number MAD-04-182. The main objective of the project was to develop an innovative electric-field sensor network based on an electro-optic field-detection technique (the Electro-optic Sensor Network, or ESN) for the performance evaluation of phased-antenna arrays at the end of their development/production cycle, and ultimately for the onsite test and calibration of deployed large-scale phased arrays.

The technical objectives during the Phase I were:

1. Feasibility study of a $1 \times N$ optical switch for ESN application.
2. Investigation comparing the performance of commercially available optical switches.
3. Review and redesign of the EO probe for the directly embedded configuration.
4. Investigation of the existing EO field-mapping system as a foundation for the optical mainframe of the anticipated ESN system.
5. Feasibility demonstration of a small scale ESN with a small number of sensors
6. Initiate the design of the control and data-acquisition software package for the ESN system.

2. Proposed Phase II Objectives

The primary objective of the Phase II MDA SBIR contract to be executed by Opteos will be the fabrication, test, and performance demonstration of a prototype linear electro-optic (EO) sensor array system to be used for the in-field characterization and calibration of the SPEAR (Scalable Panels for Efficient, Affordable Radars) Spiral 1 radar demonstrator being developed by the MDA AS (Advanced Systems) RST (Radar System Technology) panel. As such, it is expected that this network of sensors would be appropriate for rapidly conducting factory calibration, performance verification and troubleshooting measurements on the SPEAR Spiral 1 panels. An additional goal of this SBIR program is to investigate the utilization of a compact, fiber-based laser source with a compact optical network in order to allow measurements to be performed outside of the Opteos facilities, such as at the site of the radar-panel development.

Specific technical objectives of the Phase II SBIR program will include

- Expansion of the small-scale electro-optic sensor array developed during Phase I so that the prototype linear sensor array produced at the end of Phase II can cover a large number of radiating elements within an $18'' \times 44''$ antenna-array panel. In order to achieve this goal, Opteos would
 - Increase the number of EO cells in the linear array, along with the optical networks required to interconnect the cells
 - Devise effective means for interrogating a large number of parallel sensors (*e.g.*, serial vs. parallel addressing of sensors)
 - Efficiently arrange the EO sensors, for example to produce an optimum separation between sensors
 - Develop a mechanical system for scanning the EO sensor array over an antenna array
- Investigation of the effects that environment and dispersion may have on the long sections of optical fiber used to couple the optical-beam analysis components to the EO sensors

- Design and development of a compact, mobile, optical mainframe through integration of a high power, fiber-based, pulsed-laser source into the optical processing unit
- Redesign and fabrication of new optical signal distribution infrastructure through the use of faster and more efficient optical switches.
- Development of data acquisition and optical-channel-control software.
- Investigation of the most effective means for calibrating individual sensor channels to produce a uniform response across the linear sensor array.

3. Phase II Work Plan

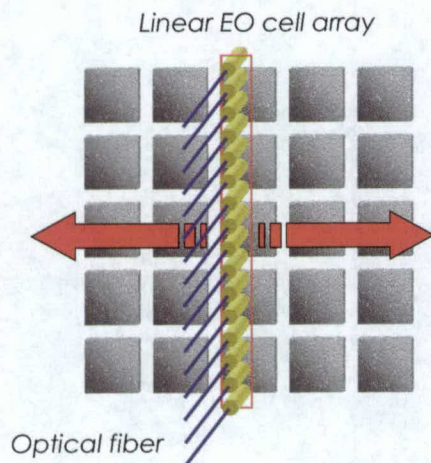


Figure 1. Concept of an electro-optic sensor linear array being scanned over a two-dimensional antenna array.

During Phase I, a small-scale ESN system with three EO sensors has been developed and its performance in a scanning embodiment has been successfully demonstrated. Compared to the feasibility demonstration performed during Phase I, a prototype ESN system produced at the end of this SBIR project would have a substantially increased number of EO sensors, allowing the flexibility to arrange the EO sensors in a variety of configurations to suit specific applications. During this SBIR, Opteos will use a linear arrangement of EO sensors in the primary design, as shown in Fig. 1. The total number of EO sensors and coverage width of the sensors would be determined by the physical size and operating frequency of a hypothetical array panel to be tested. During this SBIR, Opteos will assume that the physical dimensions of the primary array under test are sufficient to perform near-field pattern scans of two SPEAR Spiral 1 panels (18-22" \times 36-44"), as suggested by the Georgia Tech Research Institute (GTRI). Thus, the span of the EO sensor array needs to be larger than 18-22" based on the assumption that the lateral movement of the sensor array could cover the 36-44" span of the array. In addition to the physical

size of the array, the operating frequency of the array under test, which will be taken to be in X-band, will be a strong consideration in the design of the sensor array dimensions and other properties. For example, since the spacing between the EO sensors will be a half-wavelength at the highest operating frequency, it is thus approximated that 40 to 50 EO sensors may be required to form the EO sensor array for the given specification. Consideration will also be given to the most efficient design of the ESN array, and whether one sensor, multiple sensors, or even less than one sensor is required per antenna element.

With an increased number of EO sensors, it is critical to employ a high-performance optical switch with sufficient output channels, or multiple switches with a smaller number of output channels, or even a combination of optical switches and power dividers to form the required network. Fortunately, numerous optical switches and dividers with large numbers of output channels are commercially available, and Opteos will use such optical devices to form the ESN system. In addition, the speed with which one antenna array is evaluated will depend on whether each ESN element is addressed sequentially, or whether some can be interrogated in parallel. Another consideration may be whether the linear array is scanned in only one direction, or if there may be an advantage to using a series of, for example, two one-dimensional scans with a shift of sensors in the orthogonal, transverse plane in between.

In addition to the large number of EO sensors, Opteos will design and develop a new EO-mainframe, optical processing unit for the prototype ESN system during this Phase II. The proprietary EO field-mapping system that served as the predecessor of this ESN system utilized as its beam source a Ti:sapphire laser system pumped by a solid-state, cw laser that, in turn, was pumped by a diode-laser. Due

to the large physical dimension of this laser system, it is difficult and expensive to move the EO field-mapping system between laboratories and other test sites. This weakness of the EO field-mapping system must be addressed within the ESN system, since it is anticipated that the ESN system will need to be transported to locations where an array containing sensitive technology is located. We have identified that the use of a compact laser source for the ESN system would be the most important and immediate solution to achieve the required mobility for the ESN system. As a result of the Phase I effort to survey commercially available compact laser sources, Opteos has identified a fiber-based laser with specifications that satisfy all the requirements of the ESN application, once the manufacturer completes development of an RF phase-locking mechanism. With the use of this compact laser source, the ESN mainframe would have significantly smaller physical size than the mainframe used in the EO field-mapping system, making the ESN system mobile enough to be easily relocated. Not only should the fiber-based laser require less maintenance than the Ti:sapphire laser, but the cost of the fiber-based laser is approximately 50 to 60 % less than that of the Ti:sapphire laser, leading to a significant cost reduction for the complete ESN system. The mainframe will be modified to accommodate an integrated short-pulse fiber laser, as well as the different wavelength, 1.05 μm , that the new laser source will emit.

Since the fiber lengths between the optical-processing mainframe unit and the EO sensors may be somewhat longer, and may experience somewhat different environmental conditions, than those used in the R&D laboratory, Opteos will also investigate the effects that temperature, moisture, EMI, and ambient light will have on the fiber. One would typically expect that only temperature and mechanical stress would impact the inherent birefringence or possibly the attenuation of the fibers, but a variety of harsh conditions will be imposed to evaluate the need to protect the fiber and maintain its mechanical and optical integrity.

In addition to the completion of the linear EO sensor array and new mainframe hardware, Opteos will investigate means to accurately perform an initial calibration of the ESN system. Since a large number of EO sensors will be used within the ESN system, it is very important to develop a systematic effective calibration process in order to achieve uniform responsivity characteristics over all the sensor elements. Opteos is planning to use a reliable RF structure (such as a simple antenna at the desired operating frequency) to generate a calibration table containing amplitude and phase response characteristics from individual EO sensors by placing them at identical positions on the antenna. Later, this table can be automatically applied to actual measurement data through the system software. This software will be presented through an intuitive, graphical interface that controls the positioning of the ESN array, the scanning, the data acquisition and manipulation, and the quasi-real-time display of the unit-cells' amplitude and phase information.

4. Anticipated Benefits

In many military, commercial, and scientific applications, a variety of phased-array antennas are gaining popularity as high-performance RF front-ends. As the role of phased arrays increases, the need for adequate non-invasive characterization and calibration tools for those antenna arrays also increases. The Electro-optic Sensor Network (ESN) system to be developed during this SBIR program is expected to have immediate impact on a broad range of antenna array diagnostics, from early design validation to final product evaluation. In particular, the ESN system can be a very effective tool for antenna-array quality control by providing very accurate and convenient performance validation at the end of the array manufacturing process. With further development, a mobile ESN system can be used as an effective tool for the performance evaluation of field-deployed antenna arrays, as well as the evaluation of electromagnetic interactions between the antenna array and its environment. Also, by employing an embedded sensor configuration, the ESN can continuously monitor the operation and health of antenna arrays installed in remote areas. Furthermore, the outstanding flexibility of the ESN system would easily allow us to modify the system so that multiple sensors could be embedded into any RF systems in which

continuous performance monitoring is crucial. For instance, while the cellular phone industry currently employs spherical near-field ranges to measure and characterize radiation patterns of antennas, the ESN system being developed could be used to replace the RF sensors currently being used. Replacing the RF sensors with the ESN system will provide for potentially less interference, more stable measurements over temperature, fewer elements placed much closer to the antenna under test (AUT) and less interference with the AUT.

5. Transition Plans and Commercial Applications

At the end of this SBIR project, Opteos will complete the development and test of a prototype ESN system with linearly-arranged multiple EO sensors. We plan to use a compact fiber-based laser as a beam source for the system, making the system mobile so that it can be staged at the site where the array characterization needs to be performed. As a result, Opteos would have a capability to perform on-site array characterization, which may be very important at the end of array manufacturing or prior to assembly for large-scale arrays. Eventually, Opteos would develop an ESN with linear EO sensor arrays as a viable commercial product. Opteos is anticipating potential customers for the ESN system from both military and commercial array manufacturers, research institutes, and various government agencies. Also, Opteos will continue its effort to develop the ESN concept into a true embedded-sensor network so that a permanently installed ESN could continuously monitor the performance and health of critical antenna arrays.

6. Key Personnel

Dr. John F. Whitaker, Primary Investigator

Ph.D. Electrical Engineering, University of Rochester, 1988
M.Sc. Electrical Engineering, University of Rochester, 1983
B.Sc. Physics, Bucknell University, 1981

Dr. John F. Whitaker received his Ph.D. in Electrical Engineering at the University of Rochester in 1988, specializing in the area of ultrafast photonics. He joined the University of Michigan as an Assistant Research Scientist in 1989, and currently holds the titles of Research Scientist and Adjunct Professor of Electrical Engineering. Dr. Whitaker is one of co-founder of Opteos and he has served as a Vice President of the company since 2002. At the University of Michigan, Dr. Whitaker was the Coordinator for the Ultrafast Technology area in the Center for Ultrafast Optical Science between 1991 and 2002, and he was a Visiting Professor, First Class, at the University of Savoie in France in 1995. He is recognized as an expert in the fields of ultrafast optics and optoelectronics, where he has worked to open the frontier in broadband, optically-based test and measurement techniques. He has had extensive experience in the development of electro-optic and photoconductive sampling techniques for applications to the characterization of electronic materials, devices, and circuits. He has also led the effort to expand the application of electro-optic sampling to high-spatial-resolution mapping of electric fields in the near field of antennas, arrays, and circuits. Dr. Whitaker has been the author or co-author of 105 papers published in refereed journals and symposia proceedings, he has presented 15 invited papers, and he has graduated 10 Ph.D. students. He was a recipient of the IEEE Microwave Prize in 1996, as well as the College of Engineering Outstanding Research Scientist Award in 1998 and the Research Scientist Recognition Award in 2001 from the Office of the Vice President for Research, both at the Univ. of Michigan.

Selected Publications

1. J.F. Whitaker and K. Yang, "Electro-optic sampling and field mapping," book chapter in *Ultrafast Lasers, Technology and Applications*, M.E. Fermann, A. Galvanauskas, and G. Sucha, eds., pp. 473-519, Marcel Dekker AG, New York, 2003.
2. J.F. Whitaker, K. Yang, R.M. Reano, and L.P.B. Katehi, "Electro-optic probing for microwave diagnostics," invited review paper in *IEICE Trans. on Electronics*, special issue on "Recent Progress in Microwave and Millimeter-Wave Photonics Technologies" (2003).
3. R.M. Reano, K. Yang, J.F. Whitaker, and L.P.B. Katehi, "Simultaneous measurements of electric and thermal fields utilizing an electrooptic semiconductor probe," *IEEE Trans. Microwave Theory Tech.*, Vol. 49, pp. 2523-2531 (Dec. 2001).
4. R. Reano, J.F. Whitaker, and L.P.B. Katehi, "Field-tunable probe for combined electric and magnetic field measurements," *IEEE MTT-S International Microwave Symposium Digest*, New York: IEEE, pp. 1513-1516, June 2002.

7. Facilities and Equipment

During the course of this SBIR project, Opteos will access any optical equipment and microwave instrumentation not otherwise available to undertake the project through a fee-based usage arrangement with the University of Michigan. The laboratory of Dr. Whitaker in the Center for Ultrafast Optical Science at the University of Michigan is well prepared to conduct research on the ESN system, where a complete array of support instrumentation, including RF synthesizers (HP 3326A and 83732B [0.2 – 20 GHz]), an RF lock-in amplifier (Stanford Research Systems SR844), a passive 2× and active 6× multiplier, an RF Spectrum Analyzer (HP3560A), an IST-Rees Optical Spectrum Analyzer, and a PC equipped with National Instruments data acquisition hardware and software, is available for this program. During the Phase II, a compact fiber-based laser source will be acquired to develop a mobile ESN system for use with the linear sensor-array configuration. Access to microfabrication facilities for the processing of the electro-optic crystal is also available through the Solid State Electronics clean room. After initial integration and testing of the linear array of EO sensors is completed, the prototype will be integrated onto the SPEAR Spiral 1 radar demonstrator for testing at GTRI's planar NFR (near-field range) facility located in Smyrna, GA.

8. Estimated Cost

Estimated cost for the Phase II project is \$750,000.00 over the 2-year project period.

**Research
Institute**

Georgia Tech Research Institute
7220 Richardson Road
Smyrna, GA 30080

September 7, 2005

Bob Parks
U.S. Army Space and Missile Defense Command
Technical Center
P.O. Box 1500
Huntsville, AL 35807-3801

Dear Bob Parks:

GTRI believes that SBIR funding should be leveraged to develop a fully optical linear array NF scanner in parallel with the GTRI development of an RF linear array NF scanner using RST funds. Dr. Larry Corey and I recently saw some technology that NRL has developed that when coupled with the Opteos technology will provide for a fully optical transmit and receive linear array NF scanner. During a phase II SBIR with Opteos, GTRI would like to help develop this fully optical transmit/receive linear array NF scanner and demonstrate both the RF and optical linear array scanners on the spiral 1 demonstrator at the end of the phase II SBIR in about 2 years.

GTRI believes that a linear array of NF scanning probes is critical for LPD array performance. Current fielded systems such as the Terminal High-Altitude Area Defense (THAAD) radar are still under investigation for how accurately they can be recalibrated in the field after hardware replacement. The THAAD radar uses reference measurements with fixed horns around the outside edge of the array. The accuracy verified in the NFR was lower than expected. But the question of exactly how accurately it will recalibrate in the fielded environment has still not been answered. Tests have been proposed for in-field measurements to determine the repeatability of the horn to element coupling over temperature. The best test for determining the recalibration system accuracy is to measure the far-field antenna sidelobes after recalibration. Methods proposed for measuring the post recalibration far-field patterns are using a helicopter with a transmit and/or receive horn and a transmit and/or receive horn mounted on a 100 ft tower about 1 km away from the antenna. Both of these tests would cost about \$300k and would require about one week of radar time. These tests are also susceptible to errors that make it difficult to measure low sidelobes. Verification and improvement of the accuracy of this system has been an ongoing multi-million dollar effort since the early 90's. The use of a near-field scanner in the field has been partially evaluated by the contractor for this system and systems very similar and each time the engineers say they would like to use it but the development cost could not be justified. The AEGIS SPY 1 antenna used a bolt-on NF scanner on the ship and the MESAR antenna developed by Great Britain used an in-field scanning probe.

Contractor and industry interests in this technology are very high. GTRI has talked with both Raytheon and NG about using this technology to probe radar RF hardware for use in troubleshooting problems not easily measured by RF probes. The RF probes perturb the EM fields they are measuring. The optical probe would not perturb the EM fields. In addition to this interest a similar probe was developed and demonstrated by (see attached paper) NSWC/Crane and Mission Research Corp for phased array element level diagnostics (probe was embedded in radome). This probe uses a small dipole embedded in the EO cell connected to a fiber. The Opteos probe does not require the metal dipole.

Fully optical linear array NF scanner pros and cons:

Pros

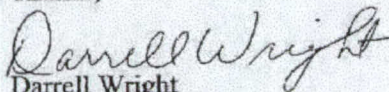
Lightweight

- 1) Less susceptible to EMI
- 2) Non-invasive measurements to the electromagnetic field
 - a) scan very near the surface which reduces the amount of overscan
 - b) potential use during operation (RF scanner could not do this)
- 3) Very fast scan of two dimensional array (scan electronically in one dimension and mechanically in other)
- 4) Potentially more stable measurements over temperature and fielded environment
- 5) Technology could be expanded to network of embedded sensors
- 6) Technology has been proven to work with single sensor in laboratory

Cons

- 1) Medium development risk (not fully developed or demonstrated in-field and with multiple sensors)
- 2) Requires a separate optical system

Thanks,



Darrell Wright
Research Engineer
Georgia Tech Research Institute